

Study of the Leaching of A Manganese Mining Residue by Na₂SO₃ in Sulfuric Acid Solution

A. Alaoui^{1 a}, K. El Kacemi^b, S. Kitane^a, K. El Ass^a

^a Laboratoire Hydrométallurgie et Environnement, ENIM B.P. 753 Rabat, Maroc

^b Laboratoire d'Electrochimie et de Chimie Analytique, Univerité Mohammed V-Agdal, Faculté des Sciences,
Rabat, Maroc

IJERT

Abstract

This work presents a party results of a study on a method of tailings management manganese mine in operation, the deposit IMINI is the largest manganese deposit in Morocco. These residues from the treatment plant pyrolusite, have a relatively fine particle size (- 710 microns) and Mn content ranging from 31.6% to 39.2%. All these residues are removed and deposited near the mine. The studied parameters were the initial concentration of Na_2SO_3 and H_2SO_4 , and solid-to-liquid ratio. Statistical techniques were used to determine that pulp density and Na_2SO_3 concentration were the most significant factors affecting the leaching kinetics and to determine the optimum conditions for dissolution. The kinetic data were analyzed with the shrinking particle and shrinking core models. A new variant of the shrinking core model (SCM) best fitted the kinetic data in which both the interfacial transfer and diffusion across the product layer affect the reaction rate. The orders of reaction with respect to $[\text{Na}_2\text{SO}_3]$, $[\text{H}_2\text{SO}_4]$ and (S/L) were 1.9, 0.8, and -2.9 respectively. The activation energy for the dissolution was found to be 54.2 kJ/mol and a semi-empirical rate equation was derived to describe the process.

1 Introduction

Manganese is an essential commodity for the steel industry, which plays an important rôle in industrial and economic development. Beneficiation of low-grade manganese ores is an area of hydrometallurgy that has been extensively studied [1], they could be of strategic international interest, but, owing to their complex nature and the morphology and peculiar surface properties of the mineral, the ore is not amenable to concentration by conventional methods such as flotation, gravity separation, magnetic treatment, etc. [2].

Manganese can be extracted from its dioxide ores either by reduction roasting followed by acid leaching or by aqueous reduction using various reducing agents. The former involves high temperature, whereas the latter can be carried out at room temperature and atmospheric pressure. Leaching experiments have been carried out using various reducing agents and acids [25, 3].

Use of SO_2 as reducing agent is encouraged by its rapid rate of reaction, low temperature operation, ease of purifying leach liquors and elimination of barren solution disposal problems [4][7]. Reductive dissolution of manganese dioxide by SO_2 is of industrial importance for the treatment of manganese [9] [10] or deep-sea manganese nodules [11][3]. Typical studies on leaching of manganese ores with SO_2 or sulfite salts are summarised in

(Tab.1).

Das et al.[14, 15] proposed a random nucleation equation for the kinetics of extraction of manganese from low-grade oxidised ores by FeSO_4 . Many studies have been carried out to leach manganese oxides and sulfide minerals simultaneously in an acid medium, H_2SO_4 or HCl . In this leaching process, the sulfide minerals function as reductants while the manganese oxides as oxidants. The sulfide minerals include galena (PbS) [16], sphalerite (ZnS) ([16, 17, 18] or zinc matt [17], pyrite (FeS_2)[19, 20, 21, 16, 22], nickel matte [17], pyriti-ferrous lignite [23].

Many studies have focused on reductive leaching of manganiferrous ores containing tetravalent manganese using organic reductants, including sawdust [24], glucose, sucrose [25, 26], lactose [26, 28], glycerine [29], oxalic acid, citric acid, tartaric acid, formic acid [30, 31], molasses in nitric acid solution [32], Molasses Alcohol Wastewater in H_2SO_4 [33] and triethanolamine and thiosulfate [34].

Aqueous SO_2 has proven to be an effective leachant because of rapid rate of dissolution, low temperatures, relative ease of purifying leach liquors and elimination of barren-solution disposal problems [42][6][43].

In the studies using low manganese ores [44, 23, 45], the rate was proposed to be controlled by SO_2 diffusion to the reaction surface, evidenced by a low apparent activation energy of 16.6 kJ/mol. Twice the stoichiometric quantity of SO_2 was required for dissolution of manganese. The $(\text{NH}_4)_2\text{SO}_3$ -bisulfite mixture at the bisulfite/ H_2SO_4 (w/w) ratio of 1:(0.52–1.55) was also used as the reductant in leaching the Fe–Mn ore concretions [47, 48]. The reaction rate was found to be first order with respect to SO_2 concentration and controlled by diffusion of SO_2 to the reaction surface [48].

Jan D. Miller and Rong-Yu Wan (1983)[47] proposed that the reduction reaction of MnO_2 in aqueous SO_2 solution is controlled by an electrochemical surface reaction and that The rate of reaction was significantly dependent on temperature. The apparent activation energy of 71.5 kJ/mol supports the conclusion that the electrochemical reaction is limited by a surface reaction mechanism. To these controversial results, the proposed model [49] seems adequate for the describe mechanism dissolution of MnO_2 by sulphite.

This work addresses the most statistically significant factors affecting the dissolution kinetics of a manganese mining residue in $\text{Na}_2\text{SO}_3/\text{H}_2\text{SO}_4$ solution. The reaction orders with respect to the process parameters were determined and a semi-

empirical rate equation was developed, a quantitative estimation of the effect of various parameters can be determined by optimization using the statistical design of experiment (DOE) technique. For this purpose, the simultaneous

effects of three control factors including Na_2SO_3 and H_2SO_4 concentration and pulp density were studied using response surface methodology (RSM).

Tab. 1: Reductive leaching of Mn ores/slimes by aqueous SO_2 /sulfite

Feed/Reagents	Conditions	Key results	Ref
MnO_2 minerals /Aq. SO_2	Studied leaching chemistry	Sulfate/dithionate ratio, depends on pH Eh and Tem.	[56, 57]
Rich Mn ore (>40% Mn)	Atm. pressure Aq. SO_2 and room temp	>95% Mn in 10 min	[9]
Low Mn ore (<40% Mn) Dithionate	Lime for neutralisation	>60% Mn, meeting ferro-manganese	[58]
Low Mn ore (<40% Mn)	Atm. pressure and room temp.	Rapid leaching rate Aq. SO_2 95% Mn recovery	[51, 52]
Low Mn ore (<40% Mn) Aq. SO_2	<60 °C controlled Eh for adding SO_2	minimised dithionate to 1g/L	[59, 60]
Low Mn slimes Dithionate		90% Mn recovery 55–60% Mn content	[61]
Fe–Mn concretions (NH_4) ₂ SO_3 –bisulfite– H_2SO_4	pH 3.5–5.5 30–70 °C	96% Mn recovery	[53]
Fe–Mn concretions	Kinetic study	E = 16,6 kJ/mol SO_2 diffusion control Aq. SO_2 First order: [SO_2]	[54]
Low Mn ores (Percolation) Aq. SO_2	Size 1.3–2.5 cm 1.5%-sat. [SO_2] 15–20 days	Rate depends on [SO_2] and pH >90% Mn recovery	[43, 61, 8]

2 Materials and methods

2.1 Materials characterization

A representative sample of residue from the the IMINI mine area of Ouarzazate Province (Morocco) was supplied by the societe Miniere (SACEM). The residu as received was thoroughly blended by rolling. Riffled samples were then collected for size distribution, chemical analysis and mineralogical characterization.

The X-ray diffraction (XRD) determination of the structures present in the product was carried out by an X'Pert Pro powder diffractometer with a vertical configuration using a power of 45 kV and a current of 40 mA. The solid products were dried at 105 °C for 24 h before each analysis. The XRD analysis of the raw product is shown on (Fig:2.1). (Tab.2) gives the chemical composition of the sample. X-ray fluorescence spectrometry has also revealed the presence of a number of trace elements such as K, Na and P. Sieve analysis of the ore is reported on (Fig:2.2). The IMINI manganese ore is characterized by the presence of a colloidal highly

hydrated MnO_2 gel, while crystalline phases include silicate gangue minerals (albite, anorthite, quartz, etc.), though a few peaks are attributable to manganese dioxide minerals (pyrolusite, psilomelane and manganomelane [45].

Tab. 2: Chemical analysis of the manganese ore

Component	Grade (%)
MnO_2	56,31
SiO_2	21,16
Al_2O_3	7,56
BaO	3,92
CaO	2,80
MgO	1,80
K_2O	1,22
Fe_2O_3	1,08
Na_2O	0,16
P_2O_5	0,04
Pb	2,04

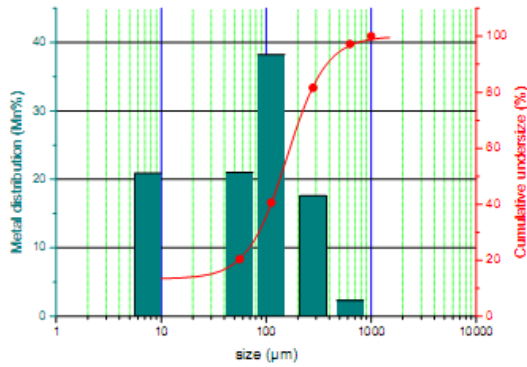


Fig. 2.2: Sieve and Chemical analysis of the manganese ore

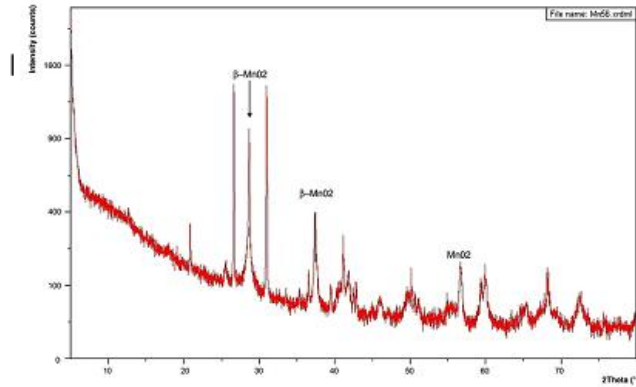


Fig. 2.1: XRD pattern of the manganese ore sample used in study.

2.2 Theoretical considerations

The Eh-pH diagrams are shown in (Fig:2:3). The S -H₂O system has been plotted without considering the sulfate species in order to be able to take account of the presence of metastable species (under ambient conditions) of importance in the leaching process, such as S₂O₃, SO₃ and HSO₃, generated by the oxidation and ionization of SO₂.H₂O [46].



By superimposing the Eh-pH diagrams of the SO₂-H₂O and Mn-H₂O systems, the stability region of manganous ion can be readily outlined in the reaction system. Ionization of the hydrogen sulfite is negligible at pH=5 or less. When the concentrations of the species derived from the

Figures 2.3 and 2.4 were traced by free Software “ChimGéné v1.3”. Examination of the Eh-pH diagram (Fig:2:3) for the Mn - H₂O system reveals that MnO₂ is very stable both in acid and alkaline solutions. To dissolve it, therefore, the environment must be reducing, so as to attain the region of stability of the manganous ion. Indeed, in the presence of sulphur dioxide, MnO₂ is attacked rapidly with the formation of manganese sulphate:

dissociation of the acid SO₂.H₂O in water are plotted as a function of pH, for a total predetermined concentration of the acid. The distribution curves for the SO₂-H₂O system are illustrated in (Fig:2.4).

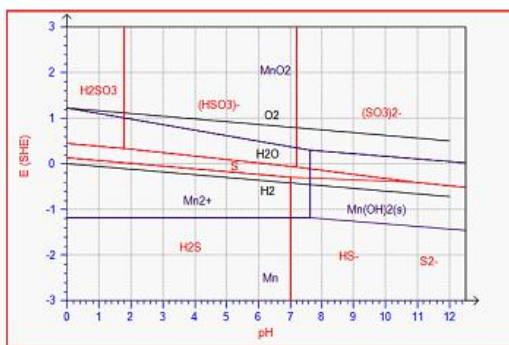


Fig. 2.3: E-pH diagram of Mn - SO₂ - H₂O system

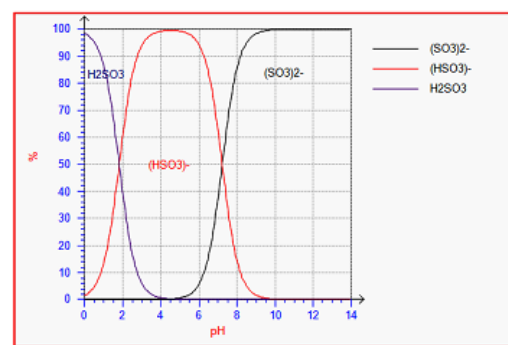


Fig. 2.4: Distribution curves of chemical species for the system SO₂ - H₂O at 25°C

2.3 Apparatus and procedures

All leaching experiments were carried out in a glass reactor double jacket equipped with a magnetically stirrer, condenser, thermometer, openings for adding the solid sample and a sampling device. This set-up provides stable hermetic conditions and allows heating at constant temperature.

The calculated quantities of H_2SO_4 and Na_2SO_3 were added to the glass reactor and heated up to the selected temperature. When the temperature was

reached and stirring speed was set, the solid (sample of residue) was added and the reaction commenced. After selected time intervals, the solution samples were taken for chemical analysis, which was carried out by UV-vis spectroscopy (Hach DR-5000) and AAS (Perkin Elmer).

Stirring was provided in 500 rpm, temperatures of 25 to 40 °C, leaching times of 1 to 15 min, while the particle size fraction leached was $\sim 630 \mu m$. The H_2SO_4 and Na_2SO_3 concentrations were in the range of 1 – 3 M and 0.32–1.0 M, respectively. The solid /liquid ratio was 67 -200 g concentrate in 1000 ml of the solution.

3 Results and discussion

3.1 Experimental design

Response surface methodology (RSM) is a collection of statistical and mathematical methods that are useful for the modeling and analyzing engineering problems. In this technique, the main objective is to optimize the response surface that is influenced by various process parameters.

Response surface methodology also quantifies the relationship between the controllable input parameters and the obtained response surfaces [35]. The design procedure of response surface methodology is as follows [36, 37]:

- 1) Designing of a series of experiments for adequate and reliable measurement of the response of interest.
- 2) Developing a mathematical model of the second order response surface with the best fittings.
- 3) Finding the optimal set of experimental parameters that produce a maximum or minimum value of response.
- 4) Representing the direct and interactive effects of process parameters through two and three dimensional plots.

If all variables are assumed to be measurable, the response surface can be expressed as follows:

$$Y = f(x_1, x_2, x_3, \dots, x_k) \quad (3.1)$$

where Y is the answer of the system, and x_i the variables of action called factors.

The goal is to optimize the response variable y. It is assumed that the independent variables are continuous and controllable by experiments with negligible errors. It is required to find a suitable approximation for the true functional relationship between independent variables and the response surface. Usually a second-order model is utilized in response surface methodology [35, 37]. In this study, the Box–Behnken experimental design was chosen for finding out the relationship between the response function (metal extracted $Y_{Mn\%}$) and variables ($[H_2SO_4]$, $[Na_2SO_3]$ and S/L).

Box–Behnken design [38, 39] is rotatable second-order designs based on three-level incomplete factorial designs. The special arrangement of the Box–Behnken design levels allows the number of design points to increase at the same rate as the number of polynomial coefficients. For three factors, for example, the design can be constructed as three blocks of four experiments consisting of a full two-factor factorial design with the level of the third factor set at zero [39].

Box–Behnken design requires an experiment number according to $N = k^2 + k + cp$, where (k) is the factor number and (cp) is the replicate number of the central point [39]. It has been applied for optimization of several chemical and physical processes [40, 41]. For the three-level three-factorial Box–Behnken experimental design, a total of 15 experimental runs, shown in (Tab.3) are needed.

Tab. 3: Parameters and their levels in the sulphite leaching experiments. Size of ore: -630 μm ; stirring speed: 500 rpm ; temperature: 298°K. time: 15 min.

Parameter	Unit	Levels and Values		
		-1	0	1
[H ₂ SO ₄]	M	1,0	2,0	3,0
[Na ₂ SO ₃]	M	0,2	0,6	1,0
S/L	g/L	67	133,5	200

The experimental plan of the leaching experiments by sulphite based on an Box-Behnken design is presented in (Tab:4). In this table, each row indicates the experimental condition of a leaching experiment. The leaching experiments were carried out in random order to avoid noise sources which had not been considered initially and which could occur during an experiment and negatively affect the results.

The responses at any condition in the interval of

our experiment design could be calculated from (Eq:3.2). Therefore, the predicted contour plots are given in (Fig:3.1). The graphic analysis (Fig:3:1(S/L.Red)) show that the Na₂SO₃ concentration and the liquid/solid ratio (S/L) were very meaningful for the dissolution of manganese. However, (Figs. 3.1(S/L.acide); (Red .Acide)) shows the limited effect of the acid in the process of dissolution of MnO₂.

Tab. 4: Experimental plan of sulphite leaching experiments based on Box-Behnken design

Experiment N°	Control factors and their levels				Y _{%Mn}	Y _{pred}
	[H ₂ SO ₄]	[Na ₂ SO ₃]	S/L			
1	1	0,2	133,5	15	15,125	
2	3	0,2	133,5	22	21,125	
3	1	1,0	133,5	52	52,875	
4	3	1,0	133,5	74	73,875	
5	1	0,6	67	85	83,375	
6	3	0,6	67	95	94,375	
7	1	0,6	200	34	34,625	
8	3	0,6	200	49	50,625	
9	2	0,2	67	40	41,500	
10	2	1,0	67	95	95,750	
11	2	0,2	200	5	4,250	
12	2	1,0	200	42	40,500	
13	2	0,6	133,5	58	58,000	
14	2	0,6	133,5	57	58,000	
15	2	0,6	133,5	59	58,000	

3.2 Statistical analysis

ANOVA analysis and the mean response calculation were performed to evaluate the effect of each factor on the optimization criteria. The main objective of ANOVA is to extract from the results how much variation each factor causes relative to the total variation observed in the rate overall manganese extraction.

For statistical analysis of the results, a mathematical function may be needed to apply to the results to meet the assumptions that makes the ANOVA valid. For this purpose, a quadratic function was considered as the best transform to be applied to the results of leaching rate. No transform was needed on the results of overall manganese extraction.

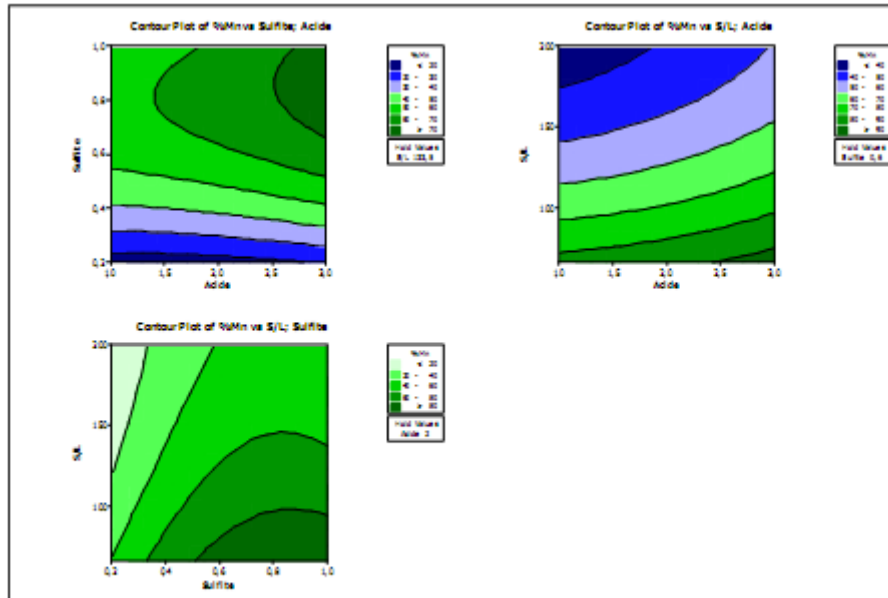


Fig. 3.1: Diagram curves iso-response for $Y_{Mn\%}$

$$Y = \beta_0 + \sum_{i=1}^n \beta_i x_i + \sum_{i=1}^n \beta_i x_i^2 + \sum_{i < j} \beta_{ij} x_i x_j + \epsilon \tag{3.2}$$

Where Y : the percentage of metal extracted, β : model coefficients, x : dimension-less coded factors for Na_2SO_3 concentration, Solid/Liquid ratio (S/L), sulphuric acid concentration and ϵ error term. The coefficients, the main effect (β_i) and two factors interactions (β_{ij}) have been estimated from the experimental results by computer simulation programming applying least square method using software MINITAB.

The results of ANOVA analysis for manganese extraction are presented in (Tab.5). In order to

eliminate the zero degree of freedom (DOF) from the error term, the pooled ANOVA was applied. Control factors with the least contribution percent were pooled.

According to this analysis, with in the 95% confidence interval, pulp density, Na_2SO_3 concentration and acid concentration were the most significant factors affecting the manganese dissolution in decreasing order. Their contributions were 49.6%, 47.4% and ~3% on manganese extraction, respectively.

Tab. 5: Pooled ANOVA for the manganese extraction

Source	DOF	Sum of squares	F_value	P_value	Contribution %
$[H_2SO_4]$	1	225,8	4,67	0,097	~ 3
$[Na_2SO_3]$	1	3591,3	74,29	0,001	47,4
S/L	1	3762,8	77,84	0,001	49,6
Error	4	193,4			
Total	7	7773,2			

Therefore, all of the factors in the model including pulp density, Na_2SO_3 and H_2SO_4 concentration, showed the statistically meaningful effect on manganese extraction (Tab.5). However, the effect of H_2SO_4 concentration ($F = 4,67$) on the reaction was not statistically meaningful. From the statistical results obtained, it was shown that the developed models Eq.(3.2) were adequate to predict the desired responses in the range of variables under study. The value of correlation coefficient (R^2) between the predicted and observed data were 0.995 for the models of manganese extraction (Fig.3.3).The main and interaction coefficients are evaluated and tested for significance by the Analysis of Variance. The coefficients significant at more than 95% confidence level on extraction of manganese are plotted in (Tab.6).

The chart (a) and the Pareto plots (b) (Fig:3.2) allow to look at both the magnitude and the importance of an effect. This chart displays the absolute value of the effects, and draws a reference line on the chart. Any effect that extends past this reference line is potentially important. The results indicate that S/L and Na_2SO_3 are significant at the 0,05 α -level. The interactions are not significant at the 0,05 α -level. The normal and Pareto plots of the effects allow to visually identify the important effects and compare the relative magnitude of the various effects. The plots confirm that S/L and Na_2SO_3 are significant at the 0,05 α -level. The adequation of Eq.(3.2) was tested by ANOVA , to see how it fitted the observations. For $\alpha=0.05$ (95% confidence level), the estimated regression Eq.(3.2) fit the experimental data adequately, see (Fig:3.3).

Tab. 6: *Test of significance of main and interaction coefficients*

Term	Coef	SE Coef	T_value	P_value
Constant	58,00	1,0083	57,523	0,000
$[\text{H}_2\text{SO}_4]$	6,75	0,6175	10,932	0,000
$[\text{Na}_2\text{SO}_3]$	22,62	0,6175	36,642	0,000
S/L	-23,12	0,6175	-37,452	0,000
$[\text{H}_2\text{SO}_4]^2$	1,50	0,9089	1,650	0,160
$[\text{Na}_2\text{SO}_3]^2$	-18,75	0,9089	-20,630	0,000
$(\text{S/L})^2$	6,25	0,9089	6,877	0,001
$[\text{H}_2\text{SO}_4] * [\text{Na}_2\text{SO}_3]$	3,75	0,8732	4,294	0,008
$[\text{H}_2\text{SO}_4] * (\text{S/L})$	1,25	0,8732	1,431	0,212
$[\text{Na}_2\text{SO}_3] * (\text{S/L})$	-4,50	0,8732	-5,153	0,004

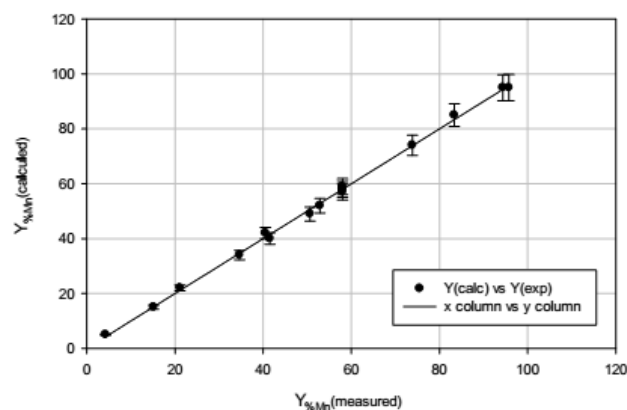
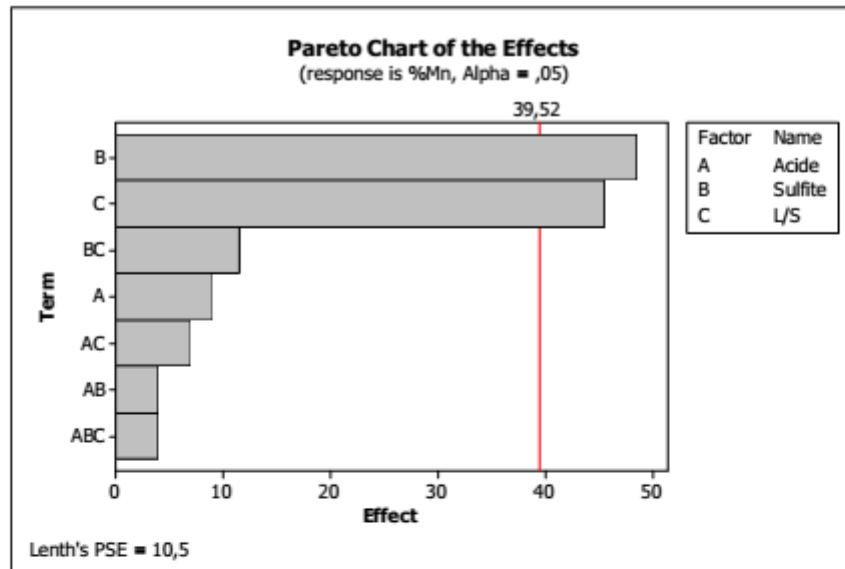
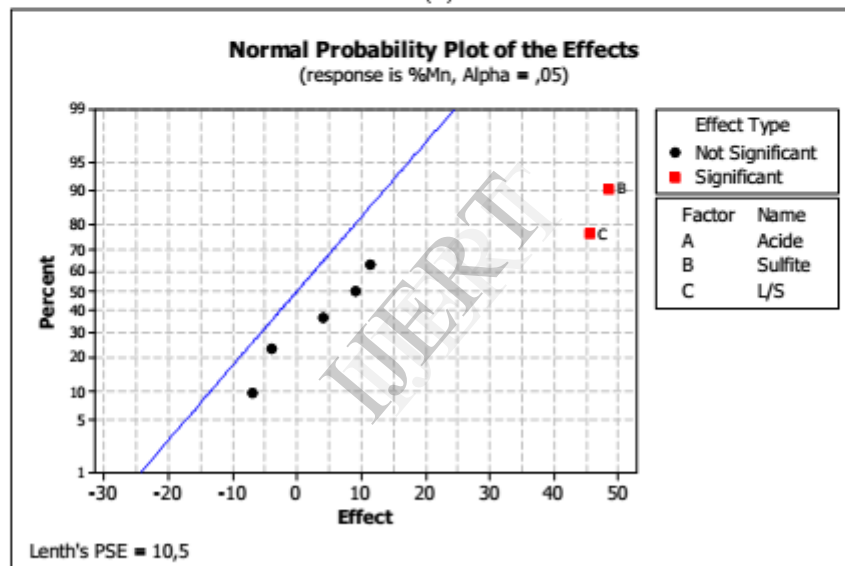


Fig. 3.3: *Correlation between $Y_{Mn\%}$ (measured) vs. $Y_{Mn\%}$ (calculated): testing the adequacy of Eq.(3.2).*



(a)



(b)

Fig. 3.2: Significant main and interaction terms for manganese extraction. (a) the Pareto chart, (b) the normal and Pareto plots.

3.3 Effect of parameters reaction

Stirring speed, solid/liquid ratio and particle size of manganese residue is selected as process variables to investigate their effects on the dissolution level of pyrolusite. In the experiments, while the effect of one parameter was studied, the values of other parameters were kept constant.

3.3.1 Effect of stirring speed

The effect of the stirring speed on the dissolution rate of pyrolusite was investigated at 0, 100, 300,

750 and 1000 rpm. The dissolution curve was given in (Fig.3.4). It can be seen from the (Fig.3.4) that the dissolution level of the process increases with increase in the stirring speed rate until about 500 rpm. The dissolution rate of pyrolusite remained almost constant at stirring speed of between 500 and 1000 rpm. Because of this, the stirring speed rate of 500 rpm was as constant value in all experiments to get guaranteed to obtain homogeneity in the batch reactor.

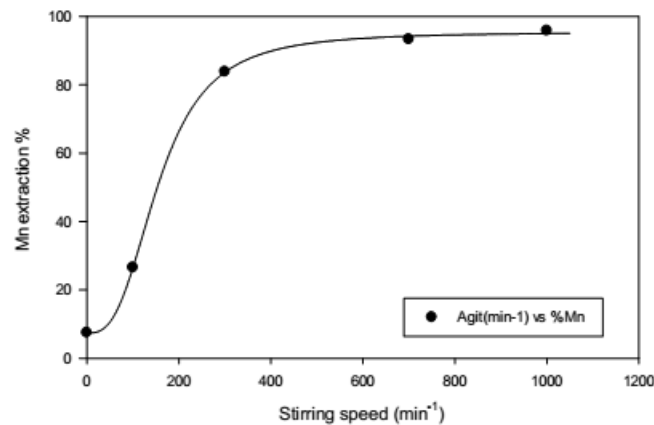


Fig. 3.4: Effect of stirring speed on dissolution rate of pyrolusite; $3M.H_2SO_4$; $1M.Na_2SO_3$; $S/L=100g/L$; $298^{\circ}K$; $15min$.

3.3.2 Effect of solid/liquid ratio

The effect of solid/liquid ratio on the dissolution rate of pyrolusite was investigated by varying ratio to 80, 100, 120, 130, 160 and 180 g/L. The

dissolution curve was given (Fig.3.5). It can be seen from (Fig.3.5) that, the dissolution rate decreases with increasing solid/liquid ratio. This situation can be explained by the decrease in the number of pyrolusite particles per amount of solutions.

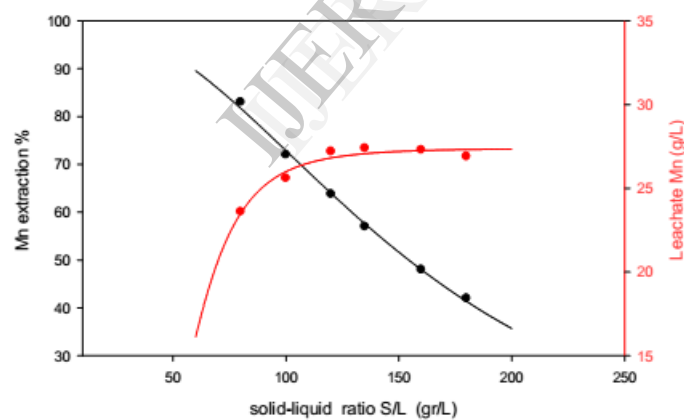


Fig. 3.5: Effect of solid/liquid ratio on dissolution rate of pyrolusite. $1M.H_2SO_4$; $0.8M.Na_2SO_3$; $298^{\circ}K$; $500min^{-1}$; $15min$.

3.3.3 Effect of particle size

The effect of particle size was studied by treating four sizes of fractions of this mineral, namely -630, -280, -125 and -63 μm . The dissolution curves are presented in (Fig.3.6). As can be seen from (Fig.3.6), as the particle size decreases the dissolution rates increased because of increasing surface area. it must also be noted that the effect of particle size is remarkably low.

3.4 Kinetic analysis

Kinetic modeling yields comprehensive information regarding leaching mechanisms. In fact, reactions involved in this process are heterogeneous in nature involving mass transport of reactant and product ions. In acidic leaching, the heterogeneous non-catalytic reaction for most manganese ore might be kinetically interpreted by using the shrinking core model (SCM) [47, 48].

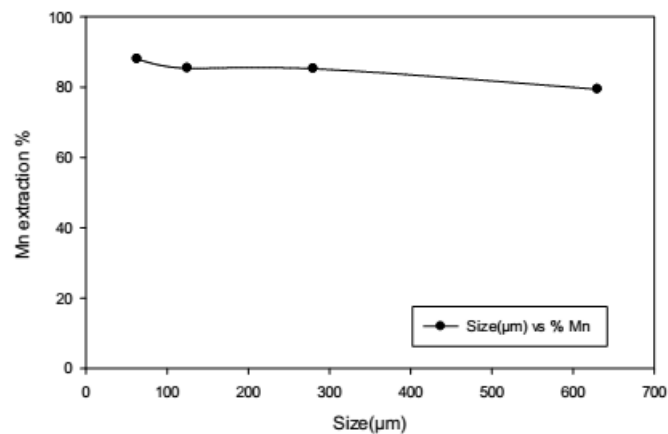
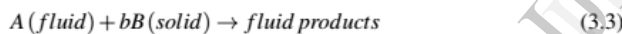


Fig. 3.6: Effect of particle size on dissolution rate. $1M.H_2SO_4$; $0.8M.Na_2SO_3$; $S/L=75g/L$; $-630\mu m$; $298^\circ K$; $500min^{-1}$; $15min$.

In the SCM model, the solid reactant is considered as non-porous particle and is initially surrounded by a fluid film through which mass transfer occurs between the solid particle and the bulk of the fluid. As the reaction proceeding, an ash/inert layer forms around the unreacted core. Detailed derivation of the shrinking core model can be found in [44].

The dissolution of pyrolusite can be expressed as follows:



The rate-limiting step, which decides the form of

$$x_B = \frac{3bk_f}{\rho_B r_0} C_A t = k'_f t \quad (3.4)$$

$$1 - 3(1 - x_B)^{2/3} + 2(1 - x_B) = \frac{6bD_e}{\rho_B r_0^2} C_A = k_d t \quad (3.5)$$

$$1 - (1 - x_B)^{1/3} = \frac{bk}{\rho_B r_0} C_A t = k_r t \quad (3.6)$$

Where k'_f , k_d and k_r are calculated from Eq.(3.4), Eq.(3.5) and Eq.(3.6), respectively.

To obtain the leaching kinetic equation, the experimental data in Figs.(3.7),(3.8) and (3.9) were transformed and fitted to Eqs.(3.4),(3.5) and (3.6). The degree of the explanation of these models on the kinetic data was evaluated using correlation coefficient (R^2) values. The slopes of these plots were used as the apparent rate constants (k'_f ; k_d and

the rate equation, may be one of the following three steps:

1. diffusion through the liquid film surrounding a solid particle,
2. diffusion through the ash/inert solid layer,
3. chemical reaction on the surface of the unreacted core.

The simplified equations of the shrinking core model when liquid film diffusion, ash/inert solid layer diffusion or the surface chemical reactions is the slowest step can be expressed as follows, respectively [44]:

k_r).

Comparing to the reaction models discussed above, a new variant of the shrinking core model suggested by Dickinson and Heal [49], provided the best fit to the kinetic data.

Based on this model, the interfacial transfer and diffusion across the product layer both affect the reaction rate. Equation of this model is given as follows:

$$\left(\frac{1}{(1-x_B)^{1/3}} - 1\right) + \frac{1}{3} \ln(1-x_B) = k_m \cdot t \quad (3.7)$$

Where x_B is the reacted fraction of pyrolusite, k_m is the apparent rate constant and t is the reaction time.

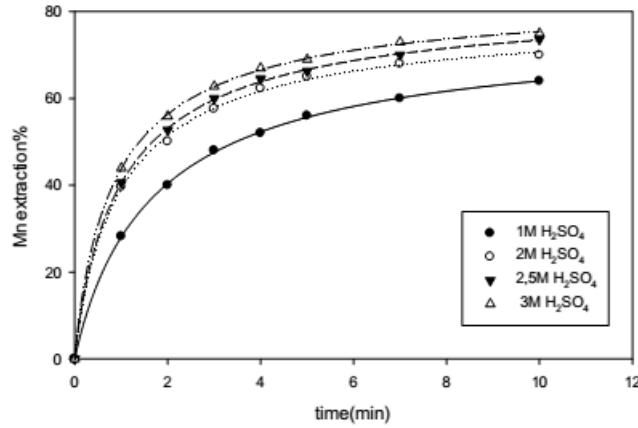


Fig. 3.7: Effect of H₂SO₄ concentration on leaching rate, [Na₂SO₃] = 0.5M; S/L = 75; 298°K

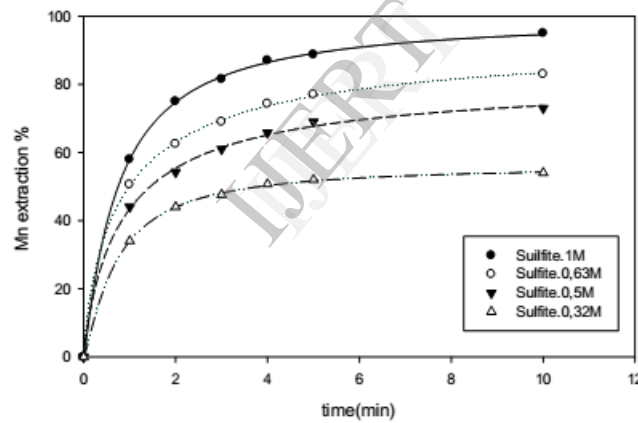


Fig. 3.8: Effect of Na₂SO₃ concentration on leaching rate, [H₂SO₄] = 2M; L/S = 13.3; 298°K

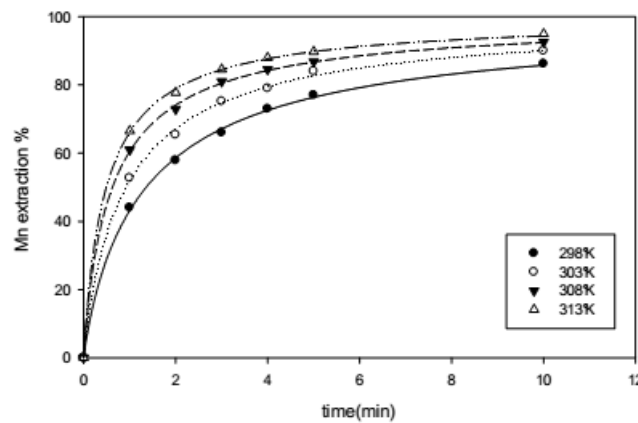


Fig. 3.9: Effect of temperature on leaching rate, [Na₂SO₃] = 1M; [H₂SO₄] = 1.5M; S/L = 75

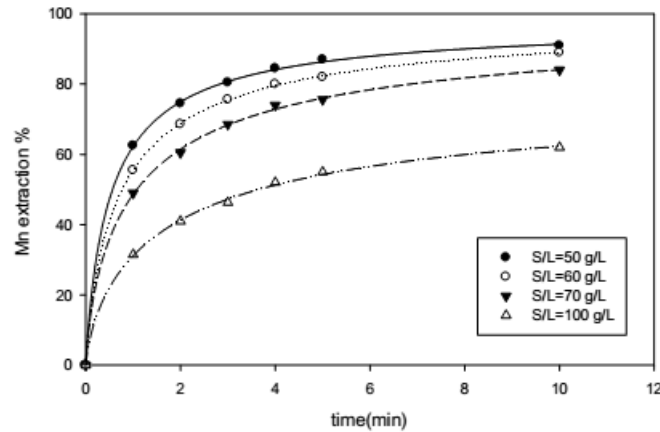


Fig. 3.10: Effect of solid-to-liquid ratio on dissolution process. $1M.H_2SO_4$; $1M.Na_2SO_3$; $298^\circ K$.

Tab. 7: Correlation coefficients (R^2) of the kinetic models in different conditions

Experimental conditions	x		$1 - (1-x)^{1/3}$		$1 - 3(1-x)^{2/3} + 2(1-x)$		$[(1-x)^{-1/3} - 1] + \frac{1}{3}\ln(1-x)$	
	k'_f	R^2	k_r	R^2	k_d	R^2	k_m	R^2
$[H_2SO_4] = 1 - 2 - 2.5 - 3M$ $[Na_2SO_3] = 0.5M$ $298^\circ K$ $L/S = 75 (g/L)$	0,0676		0,0330		0,0283		0,0075	
	0,0630	0,9136	0,0352	0,9395	0,0369	0,9634	0,0137	0,9836
	0,0632		0,0360		0,0387		0,0153	
	0,0611		0,0365		0,0412		0,0181	
$[Na_2SO_3] = 0.32 - 0.50 - 0.63 - 1M$ $[H_2SO_4] = 2M$ $298^\circ K$ $S/L = 75 (g/L)$	0,0427		0,0296		0,0182		0,0074	
	0,0616	0,9462	0,0366	0,9692	0,0411	0,9776	0,0179	0,9902
	0,0646		0,0441		0,0552		0,0291	
	0,0734		0,0654		0,0915		0,0683	
$T^\circ K = 298 - 303 - 308 - 313$ $[H_2SO_4] = 1.5M$ $[Na_2SO_3] = 1M$ $S/L = 75 (g/L)$	0,0811		0,0526		0,0634		0,0270	
	0,0811	0,9229	0,0580	0,9625	0,0769	0,9714	0,0429	0,99132
	0,0633		0,0554		0,0776		0,0590	
	0,0566		0,0565		0,0816		0,0778	
$S/L = 100 - 70 - 60 - 50 (g/L)$ $[H_2SO_4] = 1M$ $[Na_2SO_3] = 1M$ $298^\circ K$	0,0580		0,0286		0,0250		0,0079	
	0,0667	0,9002	0,0443	0,9442	0,0546	0,9627	0,0274	0,9982
	0,0644		0,0492		0,0656		0,0416	
	0,0590		0,0526		0,0741		0,0594	

As can be seen in (Tab:7), the diffusion-controlled model better fitted the kinetic data in almost all of the leaching experiments compared to the reaction-controlled model. Comparing the results of the diffusion-controlled model, Eq.(3.5), with the model, including both interfacial transfer and diffusion effects, Eq.(3.7), it is clear that the latter model better fitted the kinetic data in all of the

leaching experiments.

The variation of Eq.(3.7) with time is plotted for acid concentration, sulphite concentration, solid/liquid ratio and reaction temperature, in Figs.(3.11),(3.12), (3.13),(3.14), respectively. Using the interfacial transfer and diffusion model, the (k_m) values were plotted versus parameters difference.

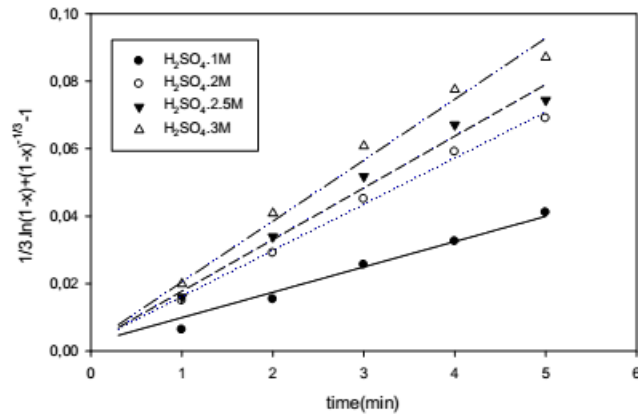


Fig. 3.11: Relationship between $[(1-x)^{-1/3} - 1] + \frac{1}{3}\ln(1-x)$ and leaching time for various H_2SO_4 concentrations. $[Na_2SO_3] = 0.5M$; $298^{\circ}K$; $S/L = 75$ g/L.

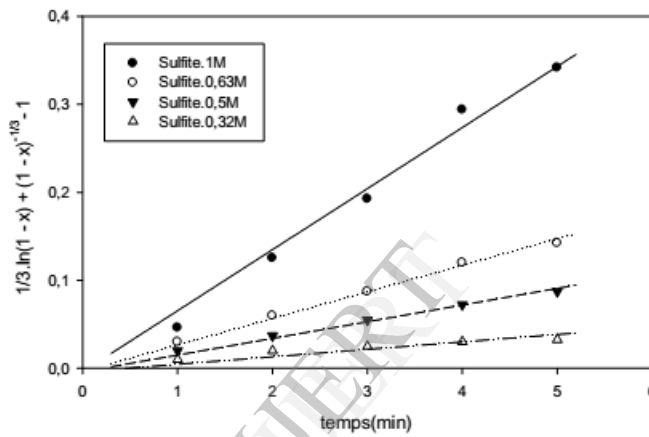


Fig. 3.12: Relationship between $[(1-x)^{-1/3} - 1] + \frac{1}{3}\ln(1-x)$ and leaching time for various Na_2SO_3 concentrations. $[H_2SO_4] = 2M$; $298^{\circ}K$; $S/L = 75$.

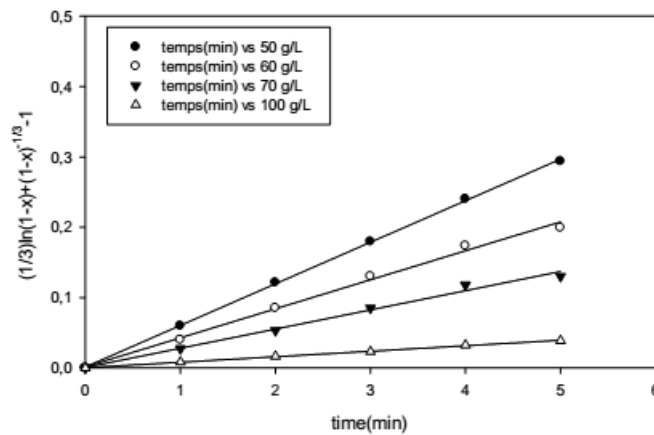


Fig. 3.13: Relationship between $[(1-x)^{-1/3} - 1] + \frac{1}{3}\ln(1-x)$ and leaching time for various solid/liqhuid ratio. $[H_2SO_4] = 1M$; $[Na_2SO_3] = 1M$; $298^{\circ}K$.

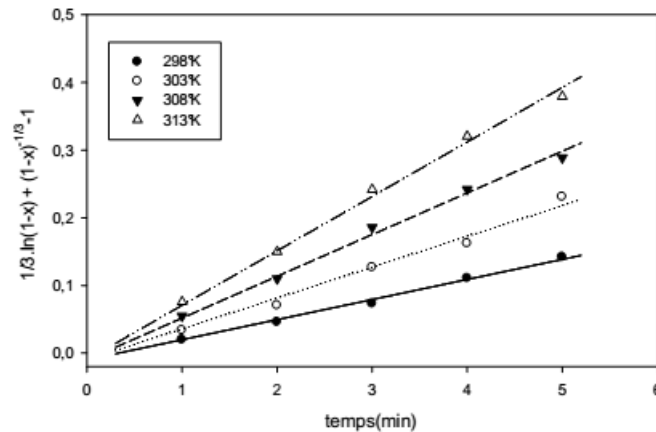


Fig. 3.14: Relationship between $[(1-x)^{-1/3} - 1] + \frac{1}{3}\ln(1-x)$ and leaching time for various temperatures. $[Na_2SO_3] = 1M$; $[H_2SO_4] = 1.5M$; $S/L = 75 g/L$.

The high linearity between (km) and acid concentration, sulphite and temperature is seen in Figs.(3.11), (3.12), (3.14) and (3.5) also shows the regression coefficient (R^2) to be found as 0.99.

$$k = A \exp\left(-\frac{E_a}{RT}\right) \quad (3.8)$$

The plot of $\ln(k_m)$ versus $(1/T)$ data for the temperatures is linear (Fig.3.15). The apparent activation energy (E_a) was, hence, determined to be (54.21 ± 4.16) kJ/mol. The value of the activation energy is high, probably because the dissolution rate of pyrolusite is controlled by the diffusion and by the mass transfer through the product layer, these two mechanisms both to control the reaction kinetics.

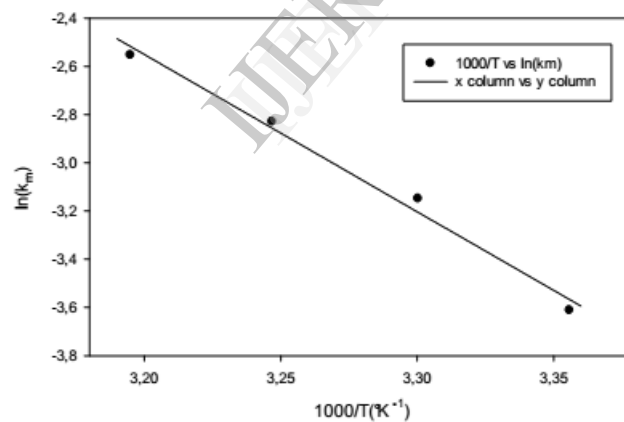


Fig. 3.15: Arrhenius plot for manganese leaching at $[Na_2SO_3] = 1M$; $[H_2SO_4] = 1.5M$; $S/L = 75 g/L$

To decide the apparent reaction order with respect to reagent concentration, the (km) values for each H_2SO_4 concentration and $[Na_2SO_3]$ and solid/liquid ratio were determined from Figs.(3.16); (3.17); (3.18) and the plots of $\log(km)$ versus $\log([H_2SO_4])$, $\log([Na_2SO_3])$ or $\log(S/L)$ were obtained. The order of reaction was found to be 0.8

with respect to H_2SO_4 concentration and 1.9 with respect to Na_2SO_3 and -2.9 for solid/liquid ratio. It seems that the leaching rate of manganese depends more on the concentration of sulphite and solid/liquid ratio.

According to Eq.(3.7), the apparent rate constant k_m can be expressed as follows:

$$k_m = k_0 [H_2SO_4]^{0.8} [Na_2SO_3]^{1.9} (S/L)^{-2.9} \cdot \exp\left(-\frac{54210}{RT}\right) \quad (3.9)$$

and $k_0 = 3,07.10^4 \text{ min}^{-1} \cdot (\text{mol/L})^{-2.7} \cdot (\text{g/L})^{2.9}$ as calculated from the provided data in (Fig:(3.15)).

By the above analysis, the kinetic model of

pyrolusite leaching by Na_2SO_3 in sulphuric acid medium is:

$$[(1-x)^{-1/3} - 1] + \frac{1}{3} \ln(1-x) = 3,07.10^4 \cdot [\text{H}_2\text{SO}_4]^{0.8} [\text{Na}_2\text{SO}_3]^{1.9} (\text{S/L})^{-2.9} \cdot \exp\left(-\frac{54210}{RT}\right) \cdot t \quad (3.10)$$

To test the agreement between the experimental conversion and the values calculated from the semi-empirical model, the graph of X_{exp} versus X_{cal} was

plotted, as shown in (Fig.3.19). It is observed that the agreement between the experimental and the calculated values is very good.

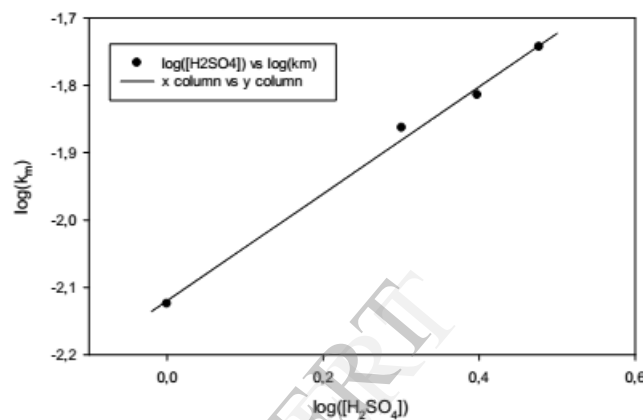


Fig. 3.16: Determination of reaction kinetic order for pyrolusite dissolution with respect to H_2SO_4 ; $[\text{Na}_2\text{SO}_3] = 0.5\text{M}$; 298°K ; $\text{S/L}=75$.

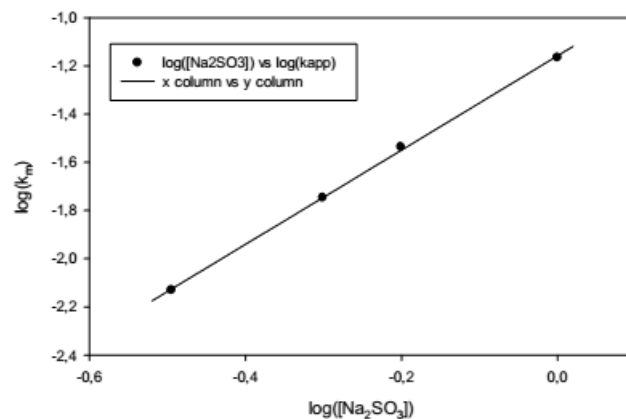


Fig. 3.17: Determination of reaction kinetic order for pyrolusite dissolution with respect to Na_2SO_3 ; $[\text{H}_2\text{SO}_4] = 2\text{M}$; $\text{S/L}=75$.

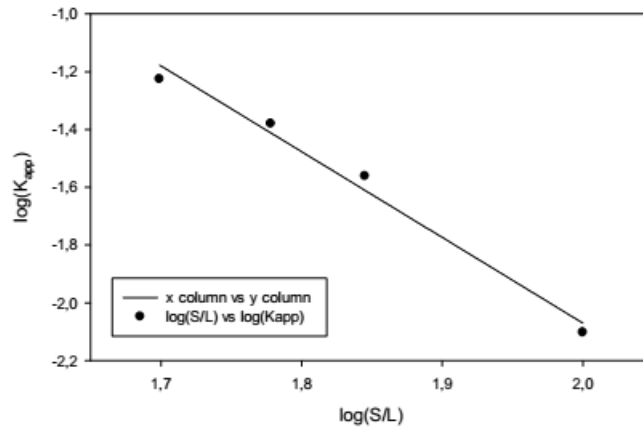


Fig. 3.18: Determination of reaction kinetic order for pyrolusite dissolution with respect to S/L ; $[Na_2SO_3] = 1M$; $[H_2SO_4] = 1M$; $298^\circ K$.

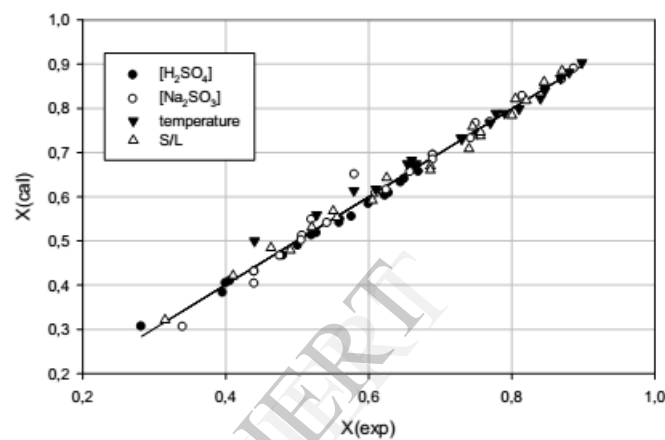


Fig. 3.19: Agreement between experimental and calculated conversion values.

4 Conclusions

The kinetic factors of the dissolution of a low grade-manganese ore in H_2SO_4/Na_2SO_3 solutions were evaluated and optimized using an response surface methodology (RSM) and a *Box-Behnken designs*. The statistical analysis performed in this study has enhanced the interpretation of kinetic data collected during the leaching studies. From the results of these studies the following conclusions can be made:

- Pulp density, Na_2SO_3 concentration and $[H_2SO_4]$ were respectively the most significant factors

$$[(1-x)^{-1/3} - 1] + \frac{1}{3} \ln(1-x) = 3,07 \cdot 10^4 \cdot [H_2SO_4]^{0,8} [Na_2SO_3]^{1,9} (S/L)^{-2,9} \cdot \exp\left(-\frac{54210}{RT}\right) \cdot t$$

- The activation energy of 54.2 kJ/mol was calculated for pyrolusite dissolution in by Na_2SO_3 in sulphuric acid medium, the kinetics study also shows strong dependence on acid, sulphite

affecting both the pyrolusite reaction rate and the manganese extraction in the confidence interval of 95%. Their contributions were 49%, 47% and ~3% on manganese extraction, respectively.

- The kinetic data best fitted a shrinking core model, in which both the interfacial transfer and diffusion through the product layer affect the reaction rate. manganese extraction of 95% was obtained after 10 min of leaching. A proper semi-empirical mathematical model expresses the dissolution rate:

concentration and S/L with a reaction order of 0.8 for total H_2SO_4 concentration and a reaction order of 1.9 for Na_2SO_3 and finally -2.9 for solid / liquid ratio.

5 References

- [1] John J.,Henn, Ralph C. Kirby, Lindsay D. Norman Jr., 1968. "Review of Major Proposed Processes for Recovering Manganese from United States Resources", U.S. Bureau of Mines, Information Circular 8368.
- [2] Massacci, P., Piga, P., Pinzari, M. and Sciotti, M., 1979. Mining and beneficiation problems related to the manganese deposits in Northern Latium. Proc. World Mining Congr., Istanbul, pp. 83-89.
- [3] S.B. Kanungo, B.R. Sant, 1974. Beneficiation of low-grade manganese ores by hydrometallurgical methods, J. Mines, Met. Fuels 6r2 173-177
- [4] P.G. Chamberlain, J.E. Pahlman, C.A., 1982. Rhoades, Recent research in leaching manganese, Paper presented at the Society of Mining Engineers, AIME Fall Meeting, Salt Lake City, UT, October 19-21, 1982, Paper 89-399.
- [5] Abbruzzese, C., 1980. Extraction of manganese from a low grade ore of Latium by reducing leaching. Boll. Assoc. Miner. Subalpina, 3-4: 592-600.
- [6] Chamberlain, P.G., Pahlman, J.E. and Rhoades, C.A., 1982. Recent research on leaching manganese. Paper presented at the Society of Mining Engineers, AIME Fall Meeting, Salt Lake City, Utah, October 19-21, Pap. 83-399.
- [7] L.D. Redden, M.T. Hepworth, R. Ben-Slimane, G.D. Welch, 1994. Recovery of manganese as carbonate after acidic leaching of Mn-Fe ores, USA, Can. Pat. Appl. CA 2,162,820 Cl. C22B 47r00 May 15, 1996, US Appl. 339,083; November 14, 1994, 25 pp
- [8] C. Abbruzzese, 1990. Percolation leaching of manganese ore by sulfur dioxide, Hydrometallurgy 25 85-97
- [9] D. Grimanelis, P. Neou-Syngouna, H. Vazarlis, 1992. Leaching of rich Greek manganese ore by aqueous solution of sulphur dioxide, Hydrometallurgy 31 139-146.
- [10] Tian, Qing-hua, Cui-yan Jiao, Xue-yi Guo, 2012. Extraction of valuable metals from manganese-silver ore. Hydrometallurgy 119-120, 8-15
- [11] Khalafalla S.E., J.E. Pahlman, 1981. Selective extraction of metals from Pacific Sea nodules with dissolved sulfur dioxide, J. Met. 33 37-42.
- [12] Kanungo S.B, R.P. Das, 1998. Extraction of metals from manganese nodules of Indian Ocean by leaching in aqueous solution of sulphur dioxide, Hydrometallurgy 20 135-146.
- [13] S.C. Das, P.K. Sahoo, P.K. Rao, 1982. Extraction of manganese from low-grade manganese ores by FeSO₄ leaching, Hydrometallurgy 8 35-47.
- [14] F. Habashi Ed. , Handbook of Extractive Metallurgy, Vol. IV, Wiley-VCH, pp. 1815.
- [15] Kholmogorov, A.G., Patrushev, V.V., Pashkov, G.L., Kononov, Y.S., Mikhlina, E.V. 1998. Reductive leaching of manganese and sulfide concentrates in sulfuric acid solutions. Zhurnal Prikladnoi Khimii (Sankt-Peterburg) 71 (11), 1890-1892.
- [16] Li, J., 2000. Effects of several factors on simultaneous leaching of zinc sulfide ore concentrates and manganese ores. Guizhou Gongye Daxue Xuebao, Ziran Kexueban 29 (3), 10-14.
- [17] Yaozhong, L., 2004. Laboratory study: simultaneous leaching silver-bearing low-grade manganese ore and sphalerite concentrate. Minerals Engineering 17 (9-10), 1053-1056.
- [18] Thomas, G., Whalley, B.J.P., 1958. The leaching of manganese from pyrolusite ore by pyrite. Canadian Journal of Chemical Engineer- ing 36, 37-43.
- [19] Gaprindashvili, V.N., Bagaturiya, L.V., Bardavelidze, M.V., Tsveniashvili, V.S., Dzhanimanov, T.B., Gogichadze, L.D., 1993. Leaching of oxidized manganese ores in mixtures with pyrite. SU Patent No. 1792995.
- [20] Omarov, N.S., Beisembaev, B.B., 1996. Use of pyrite flotation concen- trate as a reducing agent for manganese leaching from oxidized ores. Kompleksnoe Ispol'zovanie Mineral'Nogo Syr'Ya (6), 82-85.
- [21] Lu, H., Zou, X., 2001. A comprehensive utilization process for black manganese-silver ores by pyrite reducing method. Rare Metals (Beijing, China) 20 (3), 142-146.
- [22] Naik, P.K., Das, S.C., Sukla, L.B., 2002. Extraction of manganese from low-grade Nishikhal ore using pyritiferous lignite in acidic medium. Minerals & Metallurgical Processing 19 (2), 110-112.
- [23] Sanigok, U., Bayramoglu, M., 1988. Bench-scalemanganese sulfate production from lowgrade pyrolusite ores. - Part III. Chimica Acta Turcica 16 (1), 9-20
- [24] Veglio, F., Toro, L., 1994a. Reductive leaching of a concentrate manganese-dioxide ore in acid-solution— stoichiometry and preliminary kinetic-analysis. International Journal of Mineral Processing 40 (3-4), 257-272.
- [25] Veglio, F., Toro, L., 1994b. Fractional factorial-experiments in the development of manganese-dioxide leaching by sucrose in sulfuric-acid-solutions. Hydrometallurgy 36(2), 215-230.
- [26] Ali, E.A., Shahin, M.A., Ahmed, M.S., Ibrahim, I.A., 2002. Leaching of low-grade Sinai manganese ore using lactose as a reductant. Egyptian Journal of Chemistry 45 (2),359-374.
- [27] Ismail, A.A., Ali, E.A., Ibrahim, Ibrahim, A., Ahmed, M.S., 2004. A comparative study on acid leaching of low grade manganese ore using some industrial wastes as reductants. Canadian Journal of Chemical Engineering 82 (6), 1296-1300.
- [28] Arsent'ev, V.A., Yavorskaya, G.M., Kovaleva, O.V., 1991. Manganese recovery from oxide ores by leaching with acid. SU Patent No. 1624038.
- [29] Sahoo, R.N., Naik, P.K., Das, S.C., 2001. Leaching of manganese from low-grade manganese ore using oxalic acid as reductant in sulfuric acid solution. Hydrometallurgy 62 (3), 157-163.
- [30] Rodriguez, M., Rivarola, J., Ruiz, M.D., 2004. The effects of carboxylic acid addition on hydrofluoric acid autoclave leaching of a ferrocolumbite. Hydrometallurgy 74 (1-2), 39-46.
- [31] T.A. Lasheen, M.N. El Hazek, A.S. Helal, 2009. Kinetics of reductive leaching of manganese oxide ore withmolasses in nitric acid solution. Hydrometallurgy 98 (3-4) 314-317.
- [32] SU, Haifeng LIU, Huaikun WANG, Fan LÜ, Xiaoyan WEN, Yanxuan, 2010. Kinetics of Reductive Leaching of Low-grade Pyrolusite with Molasses Alcohol Wastewater in H₂SO₄. Chinese Journal of Chemical Engineering 18 (5) 730-735.

- [33] Yavorskaya, G.M., Arsentev, V.A., Kucher, V.L., Kovaleva, O.V., 1992. Redox leaching of manganese from oxide feed materials. SU Patent No. 1733492.
- [34] Kwak JS., 2005. Application of Taguchi and response surface methodologies for geometric error in surface grinding process. *Int J Machine Tools Manuf*; 45:327–34.
- [35] Kincl M, Turk S, Vrečer F., 2005. Application of experimental design methodology in development and optimization of drug release method. *Int J Pharm*. 291:39–49.
- [36] Gunaraj V, Murugan N., 1999. Application of response surface methodologies for predicting weld base quality in submerged arc welding of pipes. *J Mater Process Technol*. 88:266–75.
- [37] Box GEP, Hunter WG, Hunter JS., 1978. *Statistics for experimenters*. New York: Wiley.
- [38] Souza Anderson S, dos Santos Walter NL, Ferreira Sérgio LC., 2005. Application of Box–Behnken design in the optimization of an on-line pre-concentration system using knotted reactor for cadmium determination by flame atomic absorption spectrometry. *Spectrochimica Acta Part B*. 609:737–42.
- [39] Box GEP, Behnken DW. *Technometrics* 1960;2:195.
- [40] Annadurai G, Sung SS, Lee DL., 2004. Optimisation of floc characteristics for treatment of highly turbid water. 39:19–42.
- [41] Pahlman, J.E. and Khalafalla, S.E., 1984. Leaching of domestic manganese with dissolved SO₂. Paper presented at the Society of Mining Engineers, AIME Annual Meeting, Los Angeles, Calif., February 26–March 1.
- [42] Abbruzzese, C., Fornari, P. and Massidda, R., 1987. La lixiviation statique d'un mineral indigene demanganese par une solution de SO₂ en installation pilote. *Ind. Min., Les Tech.*; 3: 109–112.
- [43] Levenspiel, O., 1999. *Chemical Reaction Engineering*, 2nd Edition. John Wiley, New York.
- [44] Gutzmer J., Beukes NJ., Rhalmi M. & Mukhopadhyay J. 2006. Cretaceous Karstic Cave Fill Manganese-Lead-Barium Deposits of Imini, Morocco. *Economic Geology*. 101, 2, 385–405
- [45] Pourbaix, M., 1966. *Atlas of Electrochemical Equilibria*, Pergamon Press, Oxford, pp. 286–293.
- [46] Miller, J.D., Wan, R.Y., 1983. “Reaction kinetics for the leaching of MnO₂ by sulfur dioxide”, *Hydrometallurgy*, 10 (2), 219–242.
- [47] Momade, F.W.Y., Momade, Zs.G., 1999. “A study of the kinetics of reductive leaching of manganese oxide ore in aqueous methanol-sulphuric acid medium”, *Hydrometallurgy*, 54 (1), 25–39.
- [48] Dickinson, C.F., Heal, G.R., 1999. Solid–liquid diffusion controlled rate equations *Thermochim. Acta* No. 340–341, 89–103.
- [49] , P. Neou-Syngouna, H. Vazarlis, Leaching of rich Greek manganese ore by aqueous. solution of sulphur dioxide, *Hydrometallurgy* 31 1992 139–146.
- [50] Naik, P.K., Sukla, L.B., Das, S.C., 2000. Aqueous SO₂ leaching studies on Nishikhal manganese ore through factorial experiment. *Hydrometallurgy* 54 (2–3), 217–228.
- [51] Naik, P.K., Nathsarma, K.C., Das, S.C., Misra, V.N., 2003. Leaching of low-grade Joda manganese ore with sulfur dioxide in aqueous medium. *Transactions of the Institutions of Mining and Metallurgy, Section C: Mineral Processing and Extractive Metallurgy* 112 (2), C131–C134.
- [52] Svetsitskii, A.T., Nosenkov, A.N., Trunev, S.V., Dmitrevskii, B.A., Treushchenko, N.N., Yur'eva, V.I., Ivanova, N.Y., 2003. Acidic redox leaching of lean manganese ores, slimes, and dust from ferroalloy furnaces. RU Patent No. 2213155.
- [53] Partenov, D., Stefanova, V., Avramov, A., Chimbulev, M., 2004. Kinetics of leaching of polymetallic concretions in an aqueous solution of SO₂. *Izvestiya Vysshikh Uchebnykh Zavedenii, Tsvetnaya Metallurgiya* (1), 15–19.
- [54] JAN D. MILLER and RONG-YU WAN, 1983. reaction kinetics for the leaching of MnO₂ by sulfur dioxide, *Hydrometallurgy*, 10 219–242
- [55] Petrie, L.M., 1995. Molecular interpretation for SO₂ dissolution kinetics of pyrolusite, manganite and hematite, *Applied Geochemistry* 10 (3), 253–267.
- [56] Das, P.K., Anand, S., Das, R.P., 1998. Studies on reduction of manganese dioxide by (NH₄)₂SO₃ in ammoniacal medium. *Hydrometallurgy* 50 (1), 39–49.
- [57] Ravitz, S.F., Wyman, W.F., Back, A.E., Tame, K.E., 1946. The dithionate process for recovery of manganese from low-grade ores. *American Institute of Mining Metallurgical Engineers Metals Technology* 13 (No. 6, Tech. Pub. No. 2064) 10 pp.
- [58] Ward, C., Cheng, C.Y., Urbani, M.D., 2004. Manganese - from waste to high-tech material. *Publications of the Australasian Institute of Mining and Metallurgy*, pp. 241–246. 2/2004.
- [59] Ward, C.B., 2005. Acidic leaching of manganese from lean oxide ores with extraction stage for purity. WO Patent No. 2005012582.
- [60] Maslenskii, N.N., Mil'ner, R.S., Belikov, V.V., 1969. Laboratory study of dithionate treatment of three samples of low-grade manganese slimes. *Obogashchenie Rud (SanktPeterburg, Russian Federation)* 14 (2), 45.
- [61] Pahlman, J.E., Khalafalla, S.E., 1988. Leaching of domestic manganese ores with dissolved sulfur dioxide. U.S. Bureau of Mines Report of Investigations, Twin Cities, US.